Long-wavelength spin-wave energies and linewidths of the amorphous Invar alloy $Fe_{100-x}B_x$

J. A. Fernandez-Baca* and J. W. Lynn
Department of Physics, University of Maryland, College Park, Maryland 20742
and National Bureau of Standards, Gaithersburg, Maryland 20899

J. J. Rhyne
Center of Materials Science, National Bureau of Standards, Gaithersburg, Maryland 20899

G. E. Fish
Allied Signal, Inc., Morristown, New Jersey 07960
(Received 29 December 1986)

Neutron inelastic scattering experiments have been performed to investigate the long-wavelength spin dynamics of the amorphous isotropic ferromagnet $Fe_{100-x}B_x$ (for $x=14$ and 18). At both iron concentrations this system exhibits Invar behavior. The spin-wave energies are found to be well described by a quadratic dispersion relation $E=D(T)q^2+\Delta$, where $D(T)$ is the stiffness parameter and Δ is a small (~ 0.05 meV) energy gap originating primarily from dipole interactions. The stiffness parameter D renormalizes with temperature as predicted by the two-magnon interaction theory of the Heisenberg ferromagnet, although the renormalization is more dramatic than expected for short-range interactions. The $T=0$ stiffness parameters obtained from the neutron scattering measurements are 131 and 122 meV Å^2 for two samples of nominal concentration $x=14$, and 165 meV Å^2 for $x=18$. These values are almost twice as large as those derived from low-temperature magnetization measurements. It has been argued that possible mechanisms that could explain this discrepancy are the existence of additional low-lying magnetic excitations, and/or anomalous magnon linewidths that would contribute to the rapid decrease of the magnetization. Our extensive analysis of the damping of the long-wavelength spin-wave excitations in $Fe_{86}B_{14}$ has revealed that the temperature and wave-vector dependence of the spin-wave intrinsic linewidths are in good agreement with the predictions of the conventional two-magnon interaction theory of a Heisenberg ferromagnet. We therefore conclude that the discrepancy between the stiffness parameter derived from neutron scattering and magnetization measurements is likely a consequence of additional low-lying magnetic excitations, which contribute to the rather rapid renormalization of the spin-wave stiffness parameter with temperature.

I. INTRODUCTION

In this paper we report the results of our study of the wave-vector and temperature dependence of the long-wavelength spin-wave energies and intrinsic linewidths of the amorphous[1] ferromagnetic system $Fe_{100-x}B_x$ ($x=14$ and 18) by means of inelastic neutron scattering. This system exhibits an unusually large positive spontaneous volume magnetostriction that almost completely cancels the thermal expansion below the Curie temperature T_C. This cancellation is known as the Invar effect and is common to many amorphous and crystalline alloys.[2] The attraction of studying Invar systems resides in the fact that in these systems the excitation of conventional long-wavelength spin waves cannot account for the relatively rapid decrease of the bulk magnetization with temperature. In order to explain this anomaly it has been suggested that there might be additional low-lying magnetic excitations and/or some anomalously broad spin-wave excitations that might contribute to the rapid change of the magnetization. The purpose of our experiments was to probe these possibilities. Preliminary reports of this study have been published previously.[3]

We have carried out an extensive analysis of the dependence of the spin-wave linewidths Γ on the wave vector and temperature for $Fe_{86}B_{14}$. Excellent agreement was found with the prediction of the two-magnon interaction theory of a Heisenberg ferromagnet. We therefore conclude that the relatively rapid decrease of the magnetization with temperature, characteristic of the Invar alloys, should be discussed in terms of the existence of low-lying magnetic excitations in addition to the spin waves. These additional excitations apparently have a similar density of states as the spin waves since they contribute to the renormalization of the spin-wave stiffness parameter with temperature in the same manner as conventional (transverse) spin waves.

II. THEORY

The low-temperature long-wavelength elementary excitations of amorphous magnets are spin waves (or magnons[4]).[1] More properly speaking, for wavelengths λ large compared to the interatomic spacing, spin waves are approximate eigenstates of the amorphous system. In this limit of small wave vectors, all the known

theories of spin waves in isotropic ferromagnets yield the same fundamental result, a quadratic dispersion relation of the form $E=Dq^2$ which depends only on the magnitude of the wave vector **q**. For this reason, in the rest of this paper we will make reference only to the magnitude q of the wave vector. This result is general, and only the stiffness parameter D depends on the detailed atomic structure and the localized or itinerant nature of the magnetic electrons. Thus, in the long-wavelength regime, it does not seem unreasonable to assume that the well-known results of the Heisenberg model of crystalline systems should be adequate (at least as a starting point) in studying amorphous magnets. The disorder of the amorphous systems can then be introduced[5] by "smearing out" the crystal sites according to the pair correlation function $g(r)$, which represents the probability of finding two atoms separated by a distance r. This procedure has been called the "quasicrystalline approximation" (QCA),[6] "liquid model,"[7] and "virtual spherical crystal approximation."[8] In this approximation, the expression for the energy of a single long-wavelength spin wave (in the regime of small dipolar effects) is given by

$$E_q=D\left[q^2-\frac{\langle r^2\rangle}{20}q^4+\cdots\right]+2\pi\mu_B g M_0\langle\sin^2\theta\rangle\ . \quad (1)$$

In this equation D is the stiffness parameter and $\langle r^2\rangle$ is the second moment of the exchange interaction defined by

$$\langle r^2\rangle=\frac{\int J(r)g(r)r^4dr}{\int J(r)g(r)r^2dr}\ , \quad (2)$$

where $J(r)$ is the exchange interaction. The constant term in Eq. (1) is an effective (pseudo-) gap in the spin-wave dispersion relation due to dipolar interactions; θ is the polar angle of the wave vector (the z axis is defined as the direction of the spontaneous magnetization) and $\langle\sin^2\theta\rangle$ denotes the average over all magnetic domains.

Although Eq. (1) is the result for a single spin-wave excitation, it should be valid at sufficiently low temperatures where the number of spin-wave excitations is small and the eigenstates of the Heisenberg Hamiltonian are a linear superposition of noninteracting spin waves. In this "linear spin-wave" regime, the average number of spin waves $n(E_q)$ can be approximated by the Bose distribution function.

The maximum value of the magnetization $M(T)$ is obtained at $T=0$, when all the spins are aligned, and is $M(0)=g\mu_B NS/V$, where g is the gyromagnetic ratio, μ_B is the Bohr magneton, N is the number of spins in the system, and V is the volume of the sample. The creation of one spin wave results in a decrease of the total spin by one unit, and, therefore, the magnetization $M(T)$ depends (in this model) only upon the number of spin-wave excitations created at the temperature T. In the low-temperature regime, when the dispersion relation $E_q=Dq^2$ can be used in the evaluation of the population factors, the expression for the magnetization can be approximated by

$$M(T)=M(0)(1-BT^{3/2})\ , \quad (3)$$

where $M(0)$ is the magnetization at $T=0$ and

$$B=\frac{\zeta(\frac{3}{2})g\mu_B}{M(0)}\left[\frac{k_B}{4\pi D}\right]^{3/2}\ . \quad (4)$$

In this equation k_B is the Boltzmann constant and $\zeta(\frac{3}{2})$ is the Riemann ζ function [$\zeta(\frac{3}{2})=2.612$]. The inclusion of additional terms in the expansion of E_q that were neglected in obtaining Eq. (3) results in corrections in the magnetization of the order of $T^{5/2}$, $T^{7/2}$, $T^{9/2}$, etc.

The treatment of spin-wave excitations at higher temperatures is complicated since spin-wave interactions must be taken into account. States with more than one spin wave can be constructed as products of single spin-wave states, but due to the interaction between these excitations, the multiple spin-wave states are neither exact eigenfunctions of the Heisenberg Hamiltonian, nor orthogonal. In an extensive treatment of spin-wave interactions, Dyson[9] has defined two kinds of interactions (dynamic and kinetic) related to these properties of the multiple spin-wave states. The dynamic interaction is related to the fact that these multiple spin-wave states are not exact eigenfunctions and cannot diagonalize the Hamiltonian. The kinematic interaction is related to the nonorthogonality of the multiple spin-wave states; these states are overcomplete, and there must be a certain repulsion that prevents more than $2S$ spin deviations at any particular lattice point. Dyson has shown, however, that the thermodynamic effects of the kinematic interaction are negligible in any series expansion in powers of T, and, therefore, only the dynamic interaction has to be taken into account to any finite order in temperature. A similar conclusion has been reached by Marshall and Murray,[10] who used Green's function techniques to show that the kinematic interactions cancel out in the calculations of the magnetization and thermodynamic energy. The inclusion of the dynamic interaction in the treatment of the spin waves results in the renormalization of their energies and in the reduction of their lifetimes.

The renormalization of spin-wave energies with temperature in disordered ferromagnets has been studied by Huber and Sieman.[11] They showed that in these systems the expression for the renormalized spin-wave energies due to dynamic interactions can be approximated by a formula that is similar to that for crystalline systems:

$$E_q'=E_q[1-A(T)]\ , \quad (5)$$

where

$$A(T)=\frac{1}{2E_0}\sum_q E_q n(E_q)\ , \quad (6)$$

and E_q is the spin-wave energy. In this equation, E_0 is the energy of the ground state of the Heisenberg Hamiltonian. The physical meaning of the above result is that the dynamic interaction is attractive: The magnon energies are reduced by increasing the occupation numbers $n(E_q)$ since the energy required to reverse a spin is lowered if some neighbor spins are already reversed. In crystalline systems the proper evaluation of the renor-

malized spin-wave energies is possible if the spin-wave dispersion relation is known throughout the Brillouin zone. In amorphous systems, however, a well-defined Brillouin zone does not exist and a simple evaluation of the renormalized spin-wave energies can be performed only for low temperatures. In this temperature regime the occupation numbers $n(E_q)$ are significant only for small values of q, and E_q can be approximated by the quadratic dispersion relation $E_q = Dq^2$. In this regime Eq. (5) becomes

$$E_q' = E_q(1 - AT^{5/2}) , \tag{7}$$

where

$$A = \pi\zeta(\tfrac{5}{2}) \left[\frac{g\mu_B}{M_0} \right] \langle r^2 \rangle \left[\frac{k_B}{4\pi D} \right]^{5/2} . \tag{8}$$

In this equation $\zeta(\frac{5}{2})$ is the Riemann ζ function [$\zeta(\frac{5}{2}) = 1.341$] and $\langle r^2 \rangle$ is the second moment of the exchange interaction defined in Eq. (2). Although Eqs. (5)–(8) were originally derived for a Heisenberg ferromagnet, Marshall[12] has argued that similar expressions can be derived for itinerant systems. The coefficient A of the $T^{5/2}$ term of Eq. (7) is in this case more complicated, and has been calculated by Izuyama[13] for a model in which the magnetic electrons occupy a single parabolic energy band. The most striking finding of this calculation is that the coefficient A may be negative in the case of a small number of magnetic electrons.

Harris[14] has evaluated the intrinsic linewidth Γ_q of the spin waves using diagrammatic expansion techniques that account for all the two-magnon processes. In the regime $2JS \gg k_B T$ (where J is the exchange parameter for nearest neighbors) and $E_q \ll k_B T$, the spin-wave linewidth is given (to leading order in q and T) by

$$\Gamma_q(T) = \frac{1}{6} \frac{Jq^4}{8\pi^3 S} \left[\frac{k_B T}{2SJ} \right]^2 \ln^2 \frac{k_B T}{E_q} . \tag{9}$$

For a simple cubic ferromagnet the mean field theory predicts $k_B T_c = 4JS(S+1)$, and therefore the condition $2JS \gg k_B T$ means $T \ll [T_c/2(S+1)]$. However, Kashcheev and Krivoglaz[15] and Vaks *et al.*[16] have argued that Eq. (9) must hold at any temperature below the critical region, provided that the wave vector q is small enough for spin waves to be well defined, and the condition $E_q \ll k_B T$ is satisfied.

There are no calculations as yet of the spin-wave lifetime effects due to spin-wave interactions in disordered ferromagnets. However, the predicted dependence of Eq. (9) has been verified in various amorphous ferromagnets.[17–19] Besides this thermal broadening, additional broadening of the spin-wave excitations must originate from the topological disorder present in the amorphous alloys. In order to calculate the q dependence of this spin-wave broadening, one has to go beyond the "quasicrystalline approximation." Kaneyoshi[6] has reported from Green's function calculations that this linewidth $\Gamma_t(q)$ is proportional to q^7, while Singh and Roth,[20] Mano,[21] and Ishkakov[22] have predicted a leading-order q dependence of the form $\Gamma_t(q) \propto q^5$, which has the same form as the result obtained for a dilute crystalline ferromagnet. This q^5 or q^7 dependence predicted for the linewidths of the spin waves in amorphous ferromagnets, due to the topological disorder, has not been definitively observed yet, although recent results on Fe-Ni-Zr suggest that the q^5 dependence may hold.[23]

The differential cross section for the scattering of unpolarized neutrons from a system of N atoms with one localized spin per unit cell is[24]

$$\frac{d^2\sigma}{d\Omega\, dE} = A(\mathbf{k}_i, \mathbf{k}_f)[1 + n(E)] \frac{NE/\hbar}{(g\mu_B)^2} [(1 - \hat{q}_z^2)\chi_q^z F^z(q,E) + (1 + \hat{q}_z^2)\chi_q^x F^x(q,E)] . \tag{10}$$

In this equation $\mathbf{k}_i$ and $\mathbf{k}_f$ are the incident and scattered wave vectors, $\hat{q}_\alpha$ is the αth component of a unit vector parallel to $\mathbf{q}$, E is the energy transfer [$E = (\hbar^2/2m_n)(k_i^2 - k_f^2)$], χ_q^α is the isothermal susceptibility, and $F^\alpha(q,E)$ is the spectral weight function. This cross section is the sum of two terms, which we denote as longitudinal [i.e., along the direction of the magnetization (z axis)] and transverse (i.e., perpendicular to the z axis). The transverse term corresponds to the creation and annihilation of spin waves.

In the ferromagnetic regime and at small q, the transverse isothermal susceptibility is $\chi^x \propto \chi_0 q^{-2}$. However, the theory does not predict the shape of the spectral weight function $F^x(q,E)$. At low temperatures, where the spin-wave linewidths are negligible, we can approximately write

$$F^x(q,E) = \tfrac{1}{2}[\delta(E - E_q) + \delta(E + E_q)] , \tag{11}$$

where E_q is the spin-wave energy. The two terms in this spectral weight function correspond to the creation ($E > 0$) and annihilation ($E < 0$) of infinite-lifetime spin-wave excitations. At these low temperatures the longitudinal term of the cross section is expected to lead to elastic scattering only.

At higher temperatures, where the effects of spin-wave interactions must be taken into account in describing the spin dynamics, $F^x(q,E)$ is often approximated by a double Lorentzian,

$$F^x_{\mathrm{Lor}}(q,E) = \frac{1}{\pi} \left[\frac{\Gamma_q}{4(E - E_q)^2 + \Gamma_q^2} + \frac{\Gamma_q}{4(E + E_q)^2 + \Gamma_q^2} \right] , \tag{12}$$

or by a damped-harmonic-oscillator (DHO) form[25]

$$F^x_{\mathrm{DHO}}(q,E)=\frac{1}{\pi}\frac{\Gamma_q(E_q^2+\Gamma_q^2/4)}{[(E-E_q)^2+\Gamma_q^2/4][(E+E_q)^2+\Gamma_q^2/4]}\ . \tag{13}$$

We have written Eq. (13) to explicitly display the real and imaginary parts of its poles as the excitation energy (E_q) and the full width at half maximum (FWHM) linewidth (Γ_q). E_q in this equation reflects the actual physical frequency of oscillation with damping present, and corresponds to the renormalized spin-wave energy at temperature T. E_q^0, on the other hand, corresponds to the frequency at which the system would oscillate without damping. They are related via $E_q=[(E_q^0)^2-(\Gamma_q/2)^2]^{1/2}$. Note that for a mechanical oscillator $E_q^0\propto\sqrt{K/m}$, and would be independent of temperature since it is independent of damping.

At these higher temperatures the scattering associated with the longitudinal term of the cross section often has been assumed to be purely quasielastic [i.e., scattering that is strictly inelastic, but of very small energy transfer so that $F^z(q,E)$ can be approximated by a single Lorentzian centered at $E=0$], corresponding to spin diffusion. However, Vaks *et al.*[16] have suggested that at small wave vectors a much more important effect is the coupling of longitudinal fluctuations with the spin-wave modes. As a consequence of this coupling, $F^z(q,E)$ would consist of a pair of peaks at the spin-wave energies, in addition to a much smaller central peak corresponding to spin diffusion. There is, however, no conclusive experimental evidence, as yet, of propagating longitudinal modes in ferromagnetic systems.[26]

III. SPIN DYNAMICS OF INVAR ALLOYS

Inelastic neutron scattering techniques have been used successfully to study the spin dynamics of many transition-metal–based amorphous ferromagnets.[1] In all of these materials spin waves were observed at small values of q, which obey a quadratic dispersion relation of the form $E_q=D(T)q^2$. It has also been found that the spin-wave stiffness parameter $D(T)$ determined by neutron scattering renormalizes with temperature according to the two-magnon interaction prediction of Eq.(7). In addition, the low-temperature magnetization measurements usually are in agreement with Eq. (3), with a $T^{3/2}$ behavior up to $0.2-0.4T_C$ and a coefficient B which is consistent with Eq. (4), indicating that the decrease of the magnetization with temperature is due to the excitation of spin waves.

There are some amorphous systems, however, whose magnetization decreases with increasing temperature

TABLE I. Some experimental results on Fe-based amorphous ferromagnets.

System	T_C (K)	D_{SW} (meV Å^2)	D_m (meV Å^2)	D_{SW}/D_m	Remarks
$Fe_{40}Ni_{40}P_{14}B_6$	513[a]	116.9[a]	99[b]	1.2	Metglas® [c] 2826
$(Fe_{50}Ni_{50})_{75}P_{16}B_6Al_3$	482[d]	91[d]	94[d]	1.0	
$(Fe_{65}Ni_{35})_{75}P_{16}B_6Al_3$	576[d]	114[e]	115[e]	1.0	
$Fe_{70}Cr_{10}P_{13}C_7$	360[f]	60[f]	54.2[f]	1.1	
$Fe_{70}Ni_{20}Zr_{10}$	455[g]	113[g]	71.5[h]	1.6	Invar[i]
$Fe_{72}Si_{18}B_{10}$	705[j]	>230[k]	130[j]	>1.8	
$(Fe_{93}Mo_7)_{80}B_{10}P_{10}$	450[l]	85[l]	67[l]	1.3	Small Invar[m]
$Fe_{75}Si_{15}B_{10}$	710[j]	220[k]	127[j]	1.7	Invar?[j]
$Fe_{75}P_{16}B_6Al_3$	630[d]	134[d]	117[d]	1.1	Invar?[m]
$Fe_{75}P_{15}C_{10}$	597[n]	149[n]	116[n]	1.3	Invar[m]
		120[o]		1.1	
$Fe_{76}B_{24}$	723[p]	>175[q]	96[p]	>1.8	
$Fe_{80}B_{20}$	647[p]	170[r]	83[p]	2.0	Invar[s]
			92[r]	1.8	
			99[t]	1.7	
$Fe_{81}Si_9B_{10}$	662[k]	192[k]	110[j]	1.7	Invar?[j]
$Fe_{82}B_{18}$	617[q]	165[u]	71[p]	2.3	Invar[s]
$Fe_{86}B_{14}$	556[p]	118[v]	65[p]	1.8	Invar[s]
		138[q]		2.1	
		131[u]		2.0	
		122[u]		1.9	

[a]Reference 50.
[b]Reference 56.
[c]Metglas is Allied Corporation's registered trademark for amorphous alloys of metals.
[d]Reference 57.
[e]Reference 18.
[f]Reference 19.
[g]Reference 58.
[h]Reference 53.
[i]Reference 54.
[j]Reference 59.
[k]Reference 60.
[l]Reference 17.
[m]Reference 61.
[n]Reference 62.
[o]Reference 63.
[p]Reference 40.
[q]Reference 47.
[r]Reference 64.
[s]Reference 65.
[t]Reference 66.
[u]This work.
[v]Reference 31.

more rapidly than would be expected from the measured spin-wave dispersion relation. In these systems, the zero-temperature stiffness parameter D_{SW} obtained from neutron and/or Brillouin scattering techniques does not agree with the D_m value inferred from the low-temperature magnetization data and Eq. (4). Table I summarizes the main results of experiments on several Fe-based amorphous ferromagnets: Curie temperature T_C, stiffness parameters D_{SW} and D_m, and the ratio D_{SW}/D_m. These systems have been arranged in order of increasing Fe content. In many cases, the values D_{SW} and D_m were determined independently on different samples of the same nominal concentration and therefore small departures of the ratio D_{SW}/D_m from unity might be expected. A significant systematic departure of this ratio from unity is observed at the higher concentrations of Fe in alloys that are labeled as being Invar. The same kind of departure has been found in the crystalline Invar systems Fe_3Pt,[27] $Fe_{65}Ni_{35}$,[28] and $(Zr_{0.7}Nb_{0.3})Fe_2$.[29] Recently, Xianyu *et al.*[30] have also reported a strong correlation between the departure of D_{SW}/D_m from unity and the magnitude of the spontaneous volume magnetostriction that characterizes the Invar effect. It is apparent that the discrepancy between the magnetization and neutron scattering experiments may be intrinsically related to the Invar anomaly. Several attempts have been made to explain the origin of this discrepancy.

A. Anomalous spin waves

Ishikawa *et al.*[27,28,31] have proposed that the rapid demagnetization of Invar alloys with temperature is a consequence of anomalous spin-wave damping mechanisms. From their inelastic neutron scattering experiments on crystalline Fe_3Pt,[27] $Fe_{65}Ni_{35}$,[28] and amorphous $Fe_{86}B_{14}$,[31] they have suggested that the spin-wave linewidths do not obey Eq. (9), but rather follow the empirical relation

$$\Gamma_q \propto \Gamma_0(1+cT^{\alpha})q^2 , \tag{14}$$

where $\alpha \approx 1$. Thus the relatively rapid decrease of the magnetization with increasing temperature would be a consequence of the enhanced low-energy magnetic scattering produced by a combination of the anomalous linewidths and the thermal factors. We remark, however, that the proposed quadratic dependence in q for the intrinsic linewidth of the spin-wave excitations can be valid only over a relatively restricted range of q since in the hydrodynamic regime we expect $(\Gamma_q/E_q)\rightarrow 0$, as $q\rightarrow 0$.

B. Low-lying magnetic excitations

1. *Diffusive modes*

Continentino and Rivier[32] have proposed that diffusive modes originating from longitudinal spin-wave fluctuations may give rise to an additional $T^{3/2}$ term in the low-temperature magnetization of amorphous ferromagnets. They argued that the strong competition between ferromagnetic and antiferromagnetic interactions may lead to a noncollinear ground-state arrangement of spins that would result in longitudinal spin fluctuations as strong as the transverse ones. Thus, both longitudinal and transverse fluctuations would generate elementary excitations that contribute to the decrease of the magnetization with temperature. This claim was based only on the disorder of the amorphous state and did not intend to explain the anomalous demagnetization of crystalline Invar systems.

2. *Stoner excitations*

It has been proposed by Wohlfarth[33] that there are two sufficient conditions for the Invar effect to occur. The first one is the existence of weak itinerant magnetism, and the second one is the existence of strong itinerant ferromagnetism near an alloy concentration where the magnetic moment is unstable. The change of magnetization with temperature in these systems would be due to single particle (Stoner) excitations in addition to spin waves. At low temperatures, if interactions between these two kinds of excitations can be neglected, the temperature dependence of the magnetization can be written as

$$M(T)=1-(\text{spin-wave terms})-(\text{Stoner term}) . \tag{15}$$

The spin wave terms are those of Eq. (3). The Stoner term is proportional to $T^2\exp(-\Delta_S/k_BT)$ for strong ferromagnets (Δ_S is the Stoner gap) or is proportional to T^2 for weak ferromagnets.[34] Rode *et al.*,[35] Nakai *et al.*,[36] and Cochrane and Graham[37] have reported that the relation (15) holds for Fe-Ni crystalline alloys. However, Rode *et al.*[35] found that the contribution of the Stoner term was of the strong ferromagnet type, while Nakai *et al.*[36] and Cochrane and Graham[37] found that the Stoner term was of the weak type. Similar conflicting results have been reported for the Fe-B amorphous alloys: Yamada *et al.*[38] concluded that the Stoner contribution to the magnetization in $Fe_{100-x}B_x$ $(12\leq x\leq 21)$ alloys was of the weak ferromagnetic type, while Babic *et al.*[39] reported a contribution of the strong ferromagnetic type in $Fe_{80}B_{20}$ and $(Fe_xNi_{80-x})B_{18}Si_2$ $(15\leq x\leq 60)$. Furthermore, Hasegawa and Ray[40] concluded that no Stoner terms were necessary to describe the temperature dependence of the magnetization of amorphous $Fe_{100-x}B_x$ $(12\leq x\leq 28)$.

IV. EXPERIMENTAL DETAILS

A. Samples and temperature control

The samples used in this project were amorphous ribbons of Invar $Fe_{100-x}B_x$ ($x=14$ and 18), approximately 25 μm thick and 0.5 cm wide, prepared by the planar flow casting technique in vacuum.[41] Because of the high-neutron-absorption cross section of ^{10}B, boron enriched to 98.5% ^{11}B was used to prepare the Fe-B samples. In this way the overall absorption cross section was reduced by a factor of ~ 13.

The amorphous ribbons (~ 20 g each) were loosely wound between two aluminum (or copper) posts to produce flat platelike samples that were wrapped in thin aluminum (or copper) foil to improve heat transfer. The

transmission of 14.8-meV neutrons through one of the $Fe_{86}B_{14}$ samples was measured and found to be (0.75 ± 0.01). The effective transmission of the other samples was compatable.

Amorphous materials are metastable and tend to transform continuously towards more stable crystalline states. Thus, when heating amorphous samples a temperature T_x will be reached where rapid crystallization occurs, producing drastic changes in most physical properties. It is generally assumed that for $T < T_x$ amorphous alloys are stable against crystallization. However, liquid-quenched materials generally contain a tiny number of incipient crystalline nuclei from which crystal growth may proceed at temperatures far below T_x when the samples are subjected to prolonged heating. The question of how close to T_x a rapid-quenched sample can be annealed for extended periods without resulting in crystallization is an empirical matter. Arguments from crystallization kinetic data suggest that heating amorphous ribbons to temperatures up to about 100 K below T_x for several days should not result in significant crystallization.[42] In $Fe_{86}B_{14}$, where $T_x \approx 600$ K and $T_C = 556$ K (nominal values for the quoted composition), the temperature range chosen for the measurements of the spin-wave spectra was 300–500 K $(0.5-0.9T_C)$, which is adequate to probe the predictions of the spin-wave theory presented above. In this temperature range, no signs of significant crystallization (e.g., dramatic changes in the small angle scattering, or a significant increase in the stiffness parameter) were found. However, when we tried to measure the Curie temperature T_C (about 44 K below T_x) using critical scattering techniques the sample crystallized. As more measurements on this system were desired, a second sample was made of the same nominal concentration; the two samples have been labeled $Fe_{86}B_{14}$-I and $Fe_{86}B_{14}$-II. After completing the measurements of the spin-wave spectra on $Fe_{86}B_{14}$-II up to $T=520$ K without signs of significant crystallization, another attempt to measure T_C also resulted in crystallization of the sample. No attempt was made to measure T_C in $Fe_{82}B_{18}$. The nominal values of T_C and T_x for this sample are 617 and 660 K, respectively.

When measurements below room temperature were needed, the samples were attached to the copper block of a cryostat containing liquid nitrogen as a temperature bath. The combination of a variable flow cryostat with a feedback-controlled heater in the copper block allowed the temperature to be controlled within 0.1 K of the set temperature. When measurements above room temperature were made, the samples were attached to the copper block of a vacuum furnace. Two chromel-alumel thermocouples (type K) attached to the top and bottom of the sample holder allowed measurements of the temperature and temperature gradient of the sample. At 520 K the thermal gradient in the $Fe_{86}B_{14}$-II sample was <2 K, while at lower temperatures this gradient quickly became less than 1 K. A feedback-controlled heater in the copper block of the furnace allowed the temperature to be controlled within 1 K of the set temperature.

B. The neutron scattering measurements

The inelastic scattering measurements were performed on conventional triple axis spectrometers at the National Bureau of Standards Reactor (NBSR), and at the High Flux Isotope Reactor (HFIR). As mentioned earlier, the only reciprocal-lattice vector available in amorphous systems is $\tau \equiv 0$. Hence $\mathbf{Q}=\mathbf{q}$ and the measurements of the long-wavelength (small q) excitations must be taken in the small-angle scattering region, in the vicinity of the incident beam. In a small-angle scattering experiment the maximum energy that can be transferred to a neutron for a given q has an upper bound of $E_{\max} = \pm 2.88 q E_i^{1/2}$ meV, where q is in Å^{-1} and E_i is the incident energy in meV. The energy that can be transferred is then restricted to a narrow range around $E=0$.

Another feature of the small-angle scattering experiments is that the background scattering from air may become significant. The scattering from air involves processes that are strictly inelastic, but with relatively small energy transfers (quasielastic scattering) at small q. The coherent scattering amplitudes of N and O are comparable to those of the elements present in our samples. Therefore, when the mass of air M that contributes to the scattering becomes significant with respect to the mass of the sample, we might expect some additional scattering that may distort the spin-wave line shapes. It is important then to reduce the volume of air that contributes to the scattering as much as possible to improve the quality of the data. In order to accomplish this a special large-diameter ($d=68.58$ cm) vacuum furnace was built for the measurements on $Fe_{86}B_{14}$-II, where the best instrumental resolution available was utilized in order to perform a detailed study of the wave-vector and temperature dependence of the spin-wave linewidths. All the other measurements were taken with a vacuum furnace of 17.5 cm diameter.

The inelastic scattering measurements were performed with a fixed incident energy. This mode of operation allowed the placement of a pyrolytic graphite (PG) filter immediately after the monochromator. The PG filter suppresses higher-order Bragg reflections from the monochromator,[43] but the transmission of the beam through the filter produces significant small-angle scattering. The choice of the position of the filter was made to allow the neutrons to be collimated before striking the sample. A neutron monitor placed in the incident beam allowed the counting to be performed against a fixed monitor count, instead of fixed time. This counting mode avoids the necessity of corrections derived from fluctuations in the neutron flux in the reactor. Most of the experiments were performed at the BT-9 triple axis spectrometer at NBSR. In this instrument the monochromator and analyzer were PG crystals of mosaic spreads of 30′ and 45′ (FWHM). The horizontal collimations were 15′,12′,11′,25′ (FWHM in-pile, before sample, after sample, and detector positions). The vertical collimations were relaxed in order to gain signal, and were limited only by the vertical clearance of the collimator housings and possibly by the vertical size of

the monochromator, sample, and analyzer. The monochromator used in this instrument was curved about a horizontal axis in order to focus the neutron beam from the NBSR. The use of this focusing monochromator is advantageous because it makes more efficient use of the beam, although it coarsens the vertical resolution. The combination of the (002) reflection of the PG monochromator and analyzer and a fixed incident energy of 13.96 meV was selected because it provided access to an adequate range of energy transfers for our experiments, and relatively good energy resolution ($\sim$0.35 meV FWHM at the elastic position). This choice of incident energy is also far enough from 15.3 meV, where there is a large dip in the PG(002) reflectivity,[43] and allowed the measurement of energy transfers of up to 1.2 meV without making corrections for variations in the analyzer reflectivity. When a larger range of energy transfer was needed, the incident energy was fixed at 28.15 meV, where the PG filter can also be used. In this case the (004) reflection of the PG analyzer was used to improve the energy resolution (0.70 meV FWHM at the elastic position).

In order to obtain the best energy resolution without reducing the energy-transfer range accessible to the experiments, monochromator and analyzer crystals of smaller d spacings were needed. Measurements with improved energy resolution were taken at the HB-3 triple-axis spectrometer at the HFIR. In this instrument flat beryllium monochromator and analyzer crystals of small mosaic spread ($\sim$16′ FWHM) were used to study the $Fe_{86}B_{14}$-II sample. For these measurements the choice of the incident energy was 14.8 meV. Horizontal collimations of 10′ were placed before and after the sample, and the in-pile and detector collimations were 60′ each. The vertical collimations were relaxed, as explained above, but the relatively large distance between the reactor and the detector and the use of a nonfocusing monochromator resulted in substantially better vertical resolution in comparison with the BT-9 instrument. The energy resolution obtained with this arrangement was 0.22 meV (FWHM at the elastic position).

C. Data analysis

To determine the spectral shape of the inelastic scattering cross section from the experimental data the following steps were performed.

(1) The nonmagnetic inelastic background was measured and subtracted from the raw scattering data. This was a small correction which was generally energy independent.

(2) A parametrized form of the scattering cross section was chosen. The cross section was assumed to be the spin-wave cross section [transverse term of Eq. (10)] plus a δ function centered at $E=0$. The central component of the cross section represents the small-angle and incoherent scattering from the sample and environment. The spectral weight function of the spin-wave cross section was assumed to be one of the three most common forms, double δ [Eq. (11)], double Lorentzian [Eq. (12)], or damped harmonic oscillator [Eq. (13)]. The parameters of this cross section are the following. (i) The excitation energy E_q and linewidth Γ_q of the spectral weight function. (ii) An overall amplitude parameter for the inelastic peaks. By explicitly including the population factor, the spin-wave energy, and the q^{-2} dependence of the transverse isothermal susceptibility in the spin-wave cross section [Eq. (10)], this overall amplitude parameter is proportional to the number of magnetic atoms and the noninteracting susceptibility, and should be independent of q and T. (iii) An overall amplitude parameter for the central component of the cross section.

(3) A computer program was used to numerically convolute the spin-wave cross section with the (measured) four-dimensional triple-axis spectrometer resolution function.[44] The parameters of the cross section were then varied until the convoluted cross section provided the best fit (in a least-squares sense) to the data.

V. EXPERIMENTAL RESULTS

A total of 71 constant-q energy scans were obtained in the wave-vector range 0.05 Å^{-1} $\leq q \leq$ 0.14 Å^{-1}, and temperature range $0.5T_C \leq T \leq 0.94T_C$. Figure 1 shows an

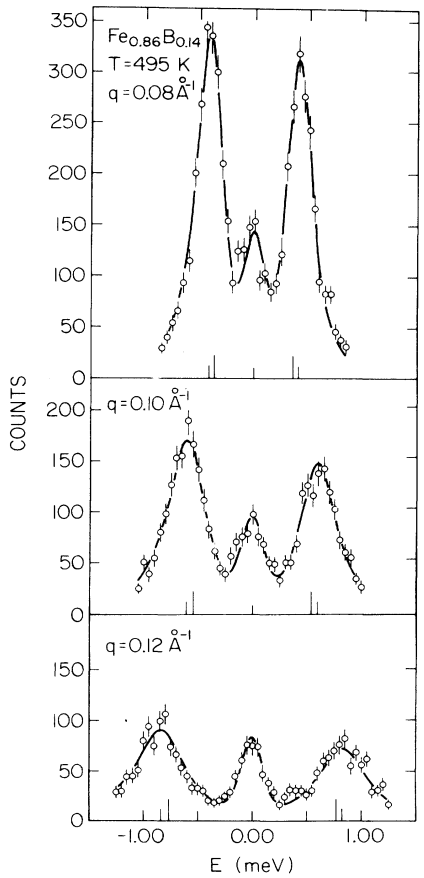

FIG. 1. Constant-q scans for $Fe_{86}B_{14}$-II at q=0.08, 0.10, and 0.12 Å^{-1}, and T=495 K. The solid curves are the result of the least-squares fits as explained in the text, using a double Lorentzian spectral weight function. An energy-independent inelastic background of five counts per point has been subtracted.

example of some inelastic scattering spectra taken at $T=495$ K on $Fe_{86}B_{14}$-II for $q=0.08$, 0.10, and 0.12 Å^{-1}. These data were obtained using beryllium monochromator and analyzer crystals, with a fixed incident energy of 14.8 meV at HFIR as explained above. The counting time was about five minutes per point. The solid curves are the result of a least-squares fit using a double-Lorentzian spectral weight function [Eq. (12)] as explained above. An excellent fit was obtained (χ^2 about one). The peaks on the energy gain ($E<0$) and energy loss $E(>0)$ sides of these spectra correspond to the annihilation and creation of spin waves. The relative intensity of these peaks is distorted due to the $(k_f^3 \cot\theta_A)$ factor in the resolution normalization.[45] This makes the intensity of the peaks on the energy-gain side appear to be higher than the intensity of the peak on the energy-loss side (k_i is fixed while k_f is varying). Because of the kinematical restrictions inherent to small-angle inelastic scattering experiments it was not always possible to scan the full line shapes.

The central peaks of the inelastic spectra are the result of small-angle and incoherent scattering from the sample, sample holder, and furnace, and are elastic but q dependent. Although this peak may contain some magnetic scattering from the sample, it was not possible to resolve this component from the nuclear scattering. For this reason no attempt was made to extract information from this region of energy.

The inelastic background has already been subtracted from the data of Fig. 1. The background was determined in the present case by making measurements with the vacuum furnace and empty sample holder in place, and then correcting for the transmission of the sample, which was measured to be 75%. The inelastic background amounted to five counts per point, independent of the energy. In the experiments on the other samples of Fe-B, which were performed with pyrolytic graphite monochromator and analyzer crystals at the NBSR, the inelastic background was measured from constant-q scans at liquid-helium temperature ($T=4.2$ K). At this temperature and for $q \geq 0.10$ Å^{-1} the spin-wave excitation energies fall outside the accessible range of energy transfer, and therefore the measurement of the intensities at the inelastic positions is a direct measurement of the background. For $q \leq 0.09$ Å^{-1}, the spin-wave excitation energies are within the accessible range of energy transfer, but the measured intensities on the energy gain side of the spectrum (~ 1 count/min) were considerably smaller than the spin-wave intensities measured at higher temperatures (≥ 100 counts/min). At this temperature the spin-wave population factors are relatively small, and the scattering from the annihilation of these excitations is too small to be measured with the tight collimations used in our experiments. For this reason the measured intensities on the energy-gain side of the spectra at this temperature were identified as the inelastic background.

In the analysis of the data, three forms of the spectral weight function for the spin-wave cross section were used: the double δ function [Eq. (11)], double Lorentzian [Eq. (12)], and the damped harmonic oscillator (DHO) [Eq. (13)]. In order to illustrate the differences between the double δ function and double Lorentzian spectral weight functions, we have plotted in Fig. 2 the results of the least-squares fits (solid curves) for $Fe_{86}B_{14}$-II at $T=495$ K for $q=0.10$ Å^{-1} for these two spectral shapes. The χ^2 values for these fits are 21.36 and 1.05, respectively. It is evident from Fig. 2(a) that there is substantial broadening that cannot be accounted by the instrumental resolution alone. Similar fits were obtained at all temperatures and wave vectors under study, indicating that the double δ spectral function is not adequate to describe the scattering cross section in our experiment. The fit to the double Lorentzian form was in all cases satisfactory, as in the case of the example shown in Fig. 2(b). This figure also shows the double Lorentzian spectral function (dashed line) before the four-dimensional convolution with the instrumental resolution function, and the intrinsic linewidth Γ_q (FWHM of the Lorentzian line shape). Typically, reliable linewidth data can be obtained when the linewidths Γ_q are greater than about 30% of the instrumental energy resolution ΔE (FWHM of the projection of the resolution function onto the energy axis at the elastic position, which in this case is 0.22 meV and is also shown in Fig. 2). Equally

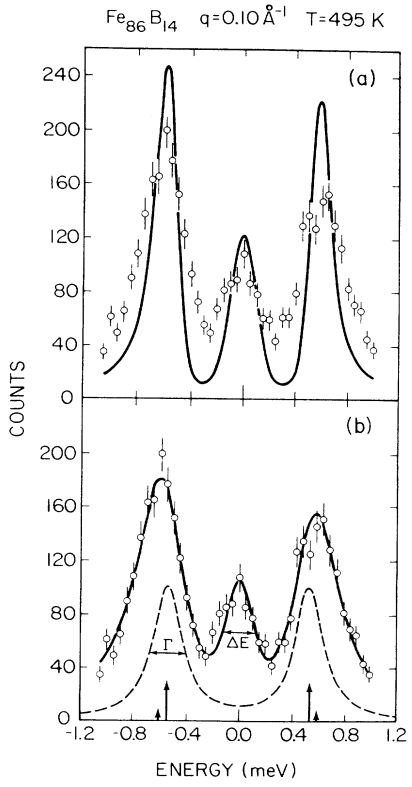

FIG. 2. Results of least-squares fits using two forms of the spectral weight function: (a) double δ function, which contains no intrinsic linewidth, and (b) double Lorentzian with linewidth Γ. The dashed curve in (b) is the double Lorentzian spectral function before the four-dimensional convolution with the instrumental resolution function. ΔE is the instrumental energy resolution (FWHM of the projection of the resolution function onto the energy axis) which is 0.22 meV.

satisfactory fits to our data were obtained with the DHO spectral shape in all cases. Furthermore, due to the fact that the spin-wave scattering intensity near the elastic position is difficult to separate from the (elastic) background scattering, it was not possible to accurately distinguish experimentally between the double Lorentzian and DHO spectral shapes.

A. Spin-waves energies

The values of the spin-wave excitation energies obtained from the least-squares fits are significantly lower than the observed positions of the peaks. This effect is due to the finite vertical resolution that makes the mean value of q greater than the nominal value at which the center of the resolution is positioned. The magnitude of these resolution corrections have been illustrated in Fig. 2(b), where arrows indicate the observed maxima of the scattering (short arrows) and the calculated spin-wave excitation energies (long arrows).

In order to study the wave-vector and temperature dependence of the spin-wave energy E_q, we have plotted E_q versus q^2 for the three samples of Fe-B at all temperatures under study. As an example, Fig. 3 shows the plot of the spin-wave energy E_q versus q^2, obtained from the Lorentzian line-shape analysis, for the $Fe_{86}B_{14}$-I sample. In all cases, the spin-wave energies obtained from the Lorentzian and DHO fits could be well described by a quadratic dispersion relation in q (plus a small energy gap) with no indication of higher-order terms. The absence of higher-order terms in q in this q range is not surprising since the largest wave vector used was $q=0.14$ Å^{-1} (for $Fe_{82}B_{18}$), which is only about 5% of the position of the first peak of the structure factor. The magnitude of the contribution of higher-order terms in the spin-wave dispersion relation can be estimated in the quasicrystalline approximation (QCA) of the Heisenberg model. From Eq. (1) it can be seen that the ratio of the quartic to quadratic terms in the dispersion relation is $R=(\frac{1}{20}q^2\langle r^2\rangle)$. If $\langle r^2\rangle$ is assumed to be of the order of $\bar{a}^2$, where $\bar{a}$ is the average nearest-neighbor distance [which in the case of $Fe_{86}B_{14}$ is $\bar{a}\approx 2.6$ Å (Ref. 46)], then for $q=0.14$ Å^{-1} we have $R\approx 6\times 10^{-3}$, i.e., the quartic term is negligible.

The energy gaps in the dispersion relation, using the double Lorentzian analysis, were ~ 0.04 meV for all three samples. This value is of the same order-of-magnitude as the pseudogap expected from dipolar interactions (the calculated dipolar pseudogap for an amorphous ribbon of $Fe_{86}B_{14}$ at $T=0$ K is $\Delta=0.07$ meV). These energies are much smaller than the instrumental energy resolution, and an accurate determination of their magnitude or temperature dependence was not possible.

It is convenient to express the results of Eq. (7), corresponding to the low-temperature spin-wave energy renormalization due to dynamic interactions, as the renormalization of the stiffness parameter D, i.e.,

$$D(T)=D(0)[1-A'(T/T_C)^{5/2}] . \tag{16}$$

In this equation $A'=AT_C^{5/2}$, where A is given in the Heisenberg model by Eq. (8). The stiffness parameters $D(T)$ were obtained from the slopes of the E_q versus q^2 curves, and then plotted against $(T/T_C)^{5/2}$. In all cases, good least-squares fits to the $T^{5/2}$ dependence of Eq. (16) could be obtained at least up to $T=0.9T_c$. Figure 4 shows, for example, the plot of D (obtained from the Lorentzian spectral weight function) versus $(T/T_c)^{5/2}$ for all samples. The results of the fits to Eq. (16) are shown as solid and dotted lines, and the values D_{SW} (the extrapolation of D to $T=0$ K) and A' obtained from the fits are listed in Table II. The agreement with this form in such a broad temperature range is remarkable, considering that this equation is obtained from a low-

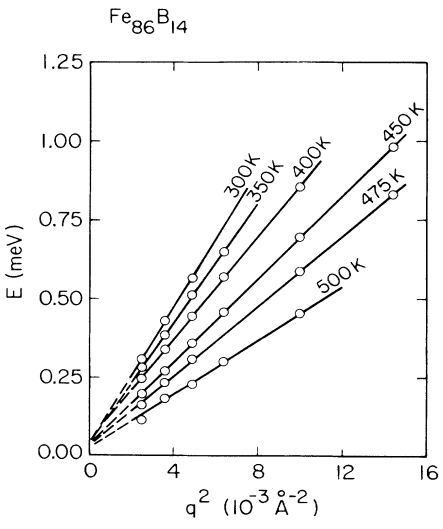

FIG. 3. E_q vs q^2 for $Fe_{86}B_{14}$-I. The values of the spin-wave energy E_q have been obtained using the double Lorentzian form of the spectral weight function.

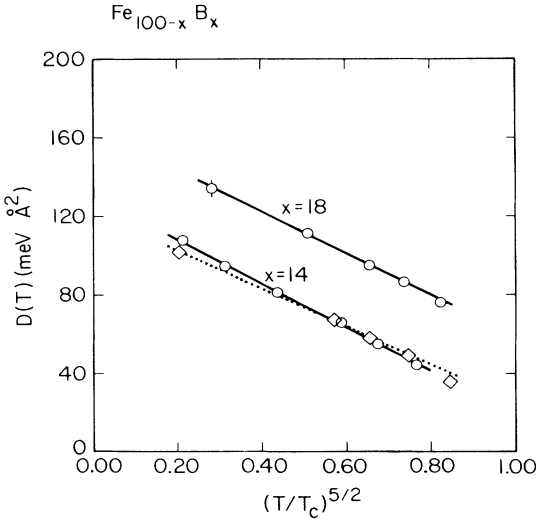

FIG. 4. D vs $(T/T_C)^{5/2}$ for $Fe_{86}B_{14}$-I (○), $Fe_{86}B_{14}$-II (◇), and $Fe_{82}B_{18}$ (○). The values of D are obtained using a double Lorentzian spectral weight function. The solid and dotted lines are the result of the least-squares fit to Eq. (16).

TABLE II. Experimental results for Fe-B.

Sample	Lorentzian fit D_{SW} (meV Å^2)	Lorentzian fit A' [a]	DHO fit D_{SW} (meV Å^2)	DHO fit A' [a]	$\langle r^2\rangle$ [b] ($\bar{a}^2$)
$Fe_{86}B_{14}$-I	130.8±2.4	0.82±0.02	124.7±2.0	0.78±0.01	17
$Fe_{86}B_{14}$-II	122.2±1.3	0.79±0.01	117.6±1.1	0.73±0.01	13
$Fe_{82}B_{18}$	165.1±1.2	0.64±0.01			17
Ni[c]					67
Permalloy[d] ($Fe_{22}Ni_{78}$)					120

[a]Coefficient A' of Eq. (16).
[b]Range of the exchange interaction defined in Eq. (2).
[c]Reference 12.
[d]Reference 48.

temperature approximation. The least-squares fits yielded values of D_{SW} of (131±2) and (122±1) meV Å^2 for $Fe_{86}B_{14}$-I and $Fe_{86}B_{14}$-II, indicating that there might be some small differences in the composition of the samples. These D_{SW} values are to be compared to 118 and 138 meV Å^2 obtained by Ishikawa *et al.*[31] and Rhyne *et al.*,[47] respectively, from previous neutron scattering experiments on samples of the same nominal composition, and a double Lorentzian cross-section analysis similar to ours.

The stiffness constant at $T=0$ K calculated from the coefficient of the $T^{3/2}$ term of the bulk magnetization measurements is $D_m=65$ meV Å^2.[40] The discrepancy between the values of D_{SW} and D_m is typical of Invar systems, and indicates that the magnetization decreases with increasing temperature more rapidly than would be expected from the measured spin-wave dispersion relation as discussed in Sec. III. The D_{SW} value obtained for $Fe_{82}B_{18}$ was (165±1) meV Å^2, which is also approximately a factor of 2 greater than the value $D_m=71$ meV Å^2 obtained from magnetization measurements.[40]

The temperature dependence of the stiffness parameter D of $Fe_{86}B_{14}$-II, obtained from the least-squares fits to the DHO spectral weight function, is illustrated in Fig. 5. In this figure the values of D from Fig. 4, obtained from the Lorentzian fits, have also been included (open squares) for comparison purposes. The values of D obtained from the slopes of the DHO excitation energy E_q versus q^2 fits (open triangles) appear to follow the $T^{5/2}$ dependence rather well in the same range as the Lorentzian values, although with a slightly different slope and smaller value of $D(0)$ (see Table II). In all cases the results obtained from the fit to the double Lorentzian and DHO spectral line shapes are qualitatively the same. For simplicity then, we present the results of our analysis primarily in terms of the double Lorentzian spectral weight function.

From the experimental values of A' and Eq. (8) we have calculated $\langle r^2\rangle$, the second moment of the effective exchange interaction defined in Eq. (2), which is an indicator of the range of the exchange interaction. These

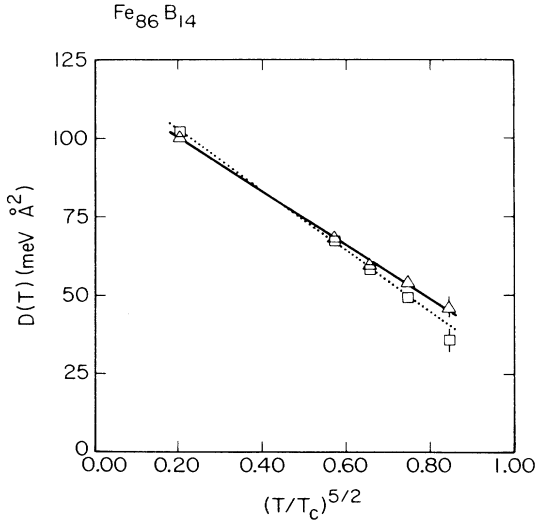

FIG. 5. D vs $(T/T_C)^{5/2}$ for $Fe_{86}B_{14}$-II. The values of D correspond to a damped harmonic oscillator (triangles) and a double Lorentzian (squares) spectral weight function analysis. The solid and dotted lines are the result of the least-squares fit to Eq. (16).

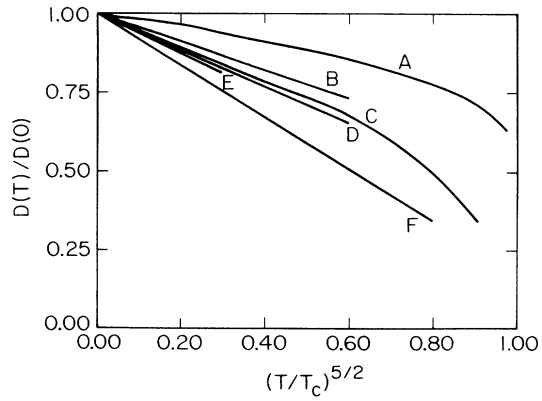

FIG. 6. $D(T)/D(0)$ vs $(T/T_C)^{5/2}$ for several ferromagnetic systems where $S\sim 1$. Curve *A*: Calculation by Bloch for a Heisenberg system with nearest-neighbor interactions (after Ref. 49). Curve *B*: $(Fe_{65}Ni_{35})_{75}P_{16}B_6Al_3$ (Ref. 18). Curve *C*: $Fe_{40}Ni_{40}P_{14}B_6$ (Metglas® 2826, Ref. 50). Curve *D*: $Fe_{70}Cr_{10}P_{13}C_7$ (Ref. 19). Curve *E*: $(Fe_{93}Mo_7)_{80}B_{10}P_{10}$ (Ref. 17). Curve *F*: $Fe_{86}B_{14}$ (this work).

values (shown in the last column of Table II for the three samples of Fe-B) are of the order of $15\bar{a}^2$, where $\bar{a}$ is the average nearest-neighbor distance obtained from diffraction experiments. These values can be compared to $67\bar{a}^2$ and $120\bar{a}^2$ obtained for crystalline Ni,[12] and Permalloy ($Fe_{20}Ni_{80}$),[48] respectively. If the Heisenberg model is applicable to these systems, the qualitative conclusion is that the range of the exchange interaction in the amorphous Fe-B alloys is significantly longer than expected for nearest-neighbor interactions, but shorter than the range for crystalline Permalloy or pure nickel.

In order to compare the range of the exchange interaction of the Fe-B and other amorphous systems, we have plotted $D/D(0)$ versus $(T/T_C)^{5/2}$ for several systems in the temperature ranges where data were available. This plot is shown in Fig. 6. Curve A is the result of the calculation performed by Bloch[49] for a cubic Heisenberg ferromagnet with nearest-neighbor interactions (i.e., $\langle r^2\rangle = a^2$, where a is the lattice parameter), and $S=1$. Curves $B-E$ show the experimental values of D on amorphous $(Fe_{65}Ni_{35})_{75}P_{16}B_6Al_3$,[18] $Fe_{40}Ni_{40}P_{14}B_6$ (Metglas® 2826),[50] $Fe_{70}Cr_{10}P_{13}C_7$ (very small Invar anomaly),[19] and $(Fe_{93}Mo_7)_{80}B_{10}P_{10}$ (small Invar anomaly).[17] Curve F shows the values of D from our experiments on Invar $Fe_{86}B_{14}$-I. In all systems we have assumed $S=1$. The values of $\langle r^2\rangle$ for the systems of curves $B-E$, calculated from Eq. (8), are $\langle r^2\rangle \leq 7\bar{a}^2$, while the corresponding value for curve F is $\langle r^2\rangle \sim 15\bar{a}^2$. The longer the range of the exchange interaction, the faster the spin-wave energies renormalize with temperature within the Heisenberg model. It also should be noted that there appears to be a relation between the steepness of the renormalization curve and the Invar effect, i.e., that amorphous Invar ferromagnets renormalize with temperature more dramatically than the non-Invar systems (A' is larger in Invar than in non-Invar systems). As a consequence of this steepness of the curve, the $T^{5/2}$ dependence of Eq. (16) is found in a rather broad range of temperatures in amorphous Invar systems: Indeed this $T^{5/2}$ dependence is expected to hold in all the temperature range (up to T_c), when the coefficient A' is one.

An interpretation of the relatively large value of the coefficient A' in these systems is that there might be additional low-lying excitations that contribute to the rather rapid decrease of D with increasing temperature. The $T^{5/2}$ dependence of D suggests that these excitations have the same form for the (energy) density of states as that for spin waves. One possibility is that these additional excitations are superimposed on the spin waves, such as has been suggested by Vaks *et al.*[16] for the coupling of longitudinal spin fluctuations with spin-wave modes. Normally, longitudinal spin fluctuations are expected to appear only at high temperatures, but there may be magnetic systems where longitudinal modes are significant at low temperatures. One possibility is a system where there is strong competition between ferromagnetic and antiferromagnetic interactions, which could lead to a noncollinear configuration of spins in the ground state. This spin configuration could have longitudinal fluctuations with amplitudes as large as the transverse ones, and would result in an additional $T^{3/2}$ temperature term in the low-temperature magnetization, explaining the $D_{SW}/D_m > 1$ anomaly found in Invar systems. Continentino and Rivier[32] have proposed the above argument as a property for amorphous systems, although it is known now that many amorphous ferromagnets do not exhibit the $D_{SW}/D_m > 1$ anomaly, while some crystalline systems ($Fe_{65}Ni_{35}$, Fe_3Pt) do. It has been suggested that the Invar systems Fe_3Pt (crystalline),[51] and Fe-Ni-Zr (amorphous),[52–54] are systems where competing interactions are important. Recently, Ishikawa has also suggested that there are additional magnetic excitations superimposed on the spin-wave excitations in crystalline $Fe_{65}Ni_{35}$.[55]

B. Spin-wave linewidths

We have also performed a detailed analysis of the wave-vector and temperature dependence of the spin-wave intrinsic linewidths for $Fe_{86}B_{14}$-II, where data with the best resolution were obtained. The object of this analysis was to probe the claim that anomalous spin-wave damping mechanisms are linked to the Invar effect. In particular, Ishikawa *et al.*[31] reported that the spin-wave linewidths in amorphous $Fe_{86}B_{14}$ and crystalline $Fe_{65}Ni_{35}$ and Fe_3Pt do not follow the conventional $q^4[T\ln(k_BT/E_q)]^2$ dependence [Eq. (9)] predicted by the two-magnon interaction theory of a Heisenberg ferromagnet, but rather follow the empirical form of Eq. (14).

Figures 7–9 show plots of the spin-wave linewidths Γ_q (FWHM of the double Lorentzian spectral weight function) of $Fe_{86}B_{14}$-II versus q at temperatures of

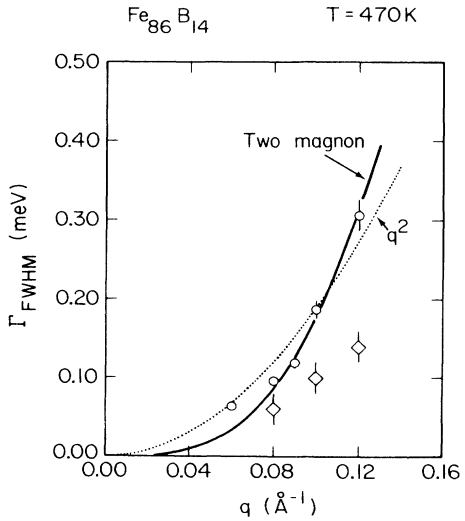

FIG. 7. Γ_q (FWHM of the Lorentzian spectral weight function) vs q for $Fe_{86}B_{14}$-II at $T=470$ K, taken with an energy resolution of 0.22 meV. The solid curve is the result of the fit to the prediction of the two-magnon interaction theory of a Heisenberg ferromagnet [Eq. (9)]. The dotted curve is the result of the fit to the empirical q^2 dependence suggested by Ishikawa *et al.* (Ref. 31). The open diamonds are the data points of Ref. 31 at $T=463$ K, taken with a much larger energy resolution of 0.60 meV.

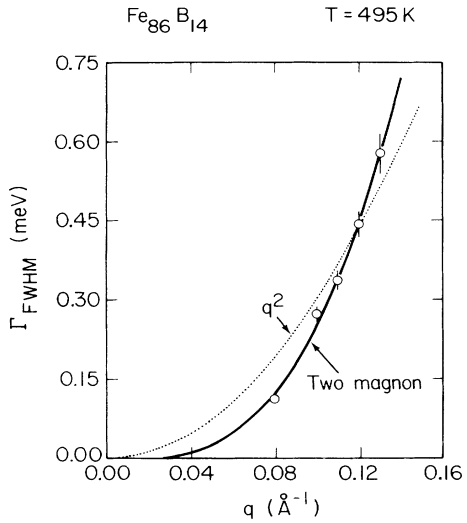

FIG. 8. Γ_q vs q for $Fe_{86}B_{14}$-II at $T=495$ K. The solid and dotted curves are the same as in Fig. 7.

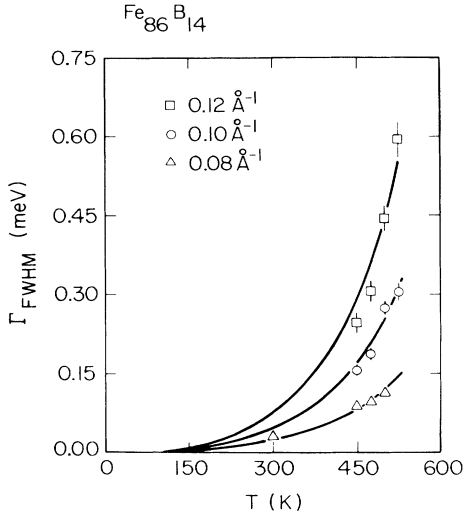

FIG. 10. Γ_q vs T for $Fe_{86}B_{14}$-II for $q=0.08$, 0.10, and 0.12 $Å^{-1}$. The solid curves are the result to the fit of the prediction of the two-magnon interaction theory of a Heisenberg ferromagnet [Eq. (9)].

$T=470$, 495, and 520 K, respectively. Also shown in Fig. 7 are the data points of Ishikawa *et al.* (open diamonds) at $T=463$ K for a sample of the same nominal concentration. The solid lines are the result of a least-squares fit to the two-magnon interaction theory result of Eq. (9), while the dotted lines are the result of a least-squares fit of our data to the empirical $\Gamma \propto q^2$ form of Eq. (14). From these figures it is evident that the two-magnon interaction prediction fits our linewidth data better than the q^2 dependence. Figure 7 also shows that our linewidth data are significantly larger than Ishikawa's at $T \approx 470$ K. However, it must be remarked that the instrumental resolution employed in our experiments was much better, and therefore we believe our data are considerably more reliable. In order to illustrate this claim we have listed the instrumental parameters in Table III. R is a number proportional to the overall volume of the resolution ellipsoid, which has been included for comparison purposes. The main information to be extracted from this table is that the overall volume of the resolution ellipsoid of our experiments on $Fe_{86}B_{14}$-II is 13.6 times smaller than the resolution employed in Ref. 31. Furthermore, all the linewidth values obtained from those data are smaller than about 25% of their instrumental energy resolution, and we believe these values are too small to obtain reliable quantitative information. In our own analysis we have discarded, as unreliable, any intrinsic linewidths smaller than about $\frac{1}{3}E_{\rm res}$.

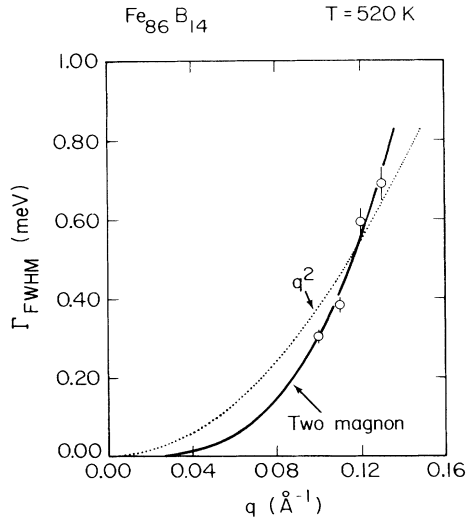

FIG. 9. Γ_q vs q for $Fe_{86}B_{14}$-II at $T=520$ K. The solid and dotted curves are the same as in Figs. 7 and 8.

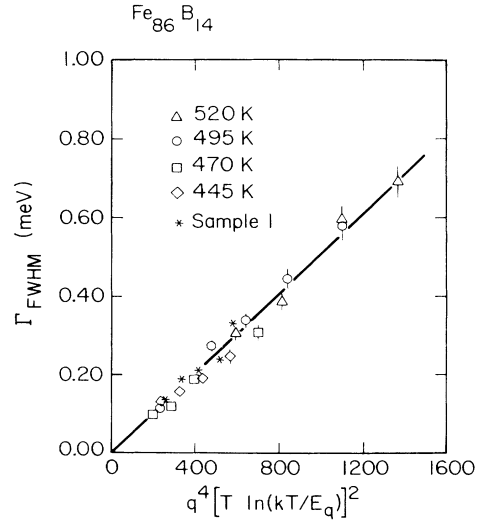

FIG. 11. Γ_q (FWHM of the Lorentzian spectral weight function) vs $q^4[T\ln(k_BT/E_q)]^2$ for $Fe_{86}B_{14}$-II. The solid curve is the result of a fit to the prediction of the two-magnon interaction theory of a Heisenberg ferromagnet [Eq. (9)]. The asterisks are the linewidths for $Fe_{86}B_{14}$-I.

TABLE III. Comparison of the instrumental parameters of three neutron inelastic scattering experiments on amorphous $Fe_{86}B_{14}$.

Parameter	Experiment[a] at HFIR	Experiment[a] at NBSR	Experiment of Ref. 31
Fixed E_i (meV)	14.8	13.98	14.5
Monochromator	Be(101)	PG(002)	PG(002)
Analyzer	Be(002)	PG(002)	PG(002)
E resolution (meV)[b]	0.22	0.35	0.60[c]
Vertical resolution ($Å^{-1}$)	0.1	0.2	0.2[c]
R[d]	1.0	5.2	13.6[c]

[a]This work.
[b]FWHM at elastic position.
[c]Estimated.
[d]Number proportional to the overall volume of the resolution ellipsoid.

Figure 10 shows the temperature dependence of our linewidth data for $q=0.08$, 0.10, and 0.12 $Å^{-1}$. The solid line is the result of the least-squares fit to the two-magnon interaction theory of Eq. (9). Our linewidth data are in good agreement with this prediction, and there are no indications of the almost linear dependence in T of Eq. (14).

A better overview of the wave vector and temperature dependence of the spin-wave intrinsic linewidths can be obtained by plotting Γ_q versus $q^4[T\ln(k_BT/E_q)]^2$ as shown in Fig. 11. This figure contains our linewidth data for $Fe_{86}B_{14}$-II at $T=445$, 470, 495, and 520 K, for values of q between 0.08 and 0.13 $Å^{-1}$. The solid line is the result of the fit to the two-magnon interaction form [Eq. (9)], which is seen to agree with our linewidth data in the entire range of T and q under study. Also included in Fig. 11, for comparison purposes, are the linewidth data from our $Fe_{86}B_{14}$-I sample (asterisks), which are in good agreement with the data for $Fe_{86}Be_{14}$-II, taken with better resolution. The slope of the solid line of Fig. 11 is $(0.506\pm0.009)\times10^{-3}$ meV $Å^4K^{-2}$, which is about 38% lower than the slope for amorphous $(Fe_{65}Ni_{35})_{75}P_{16}B_6Al_3$ (of comparable Curie temperature and stiffness parameter) obtained by Tarvin *et al.* (see Fig. 4 of Ref. 18, corresponding to the plot of the half width at the half maximum (HWHM) linewidths versus $q^4[\ln^2(k_BT/E_q)]$).

In order to illustrate that the results of Fig. 11 are not dependent on the form of the spectral weight function used in the analysis, we have plotted the linewidths obtained from the fits to the DHO spectral weight function versus $q^4[T\ln(k_BT/E_q)]^2$ in Fig. 12. An equally good fit is obtained, but with a slighter smaller slope of 0.480×10^{-3} meV $Å^4K^{-2}$.

The parametrization of the scattering cross section included an overall amplitude parameter for the inelastic spin-wave scattering spectra as described in Sec. II. As expected, this amplitude parameter was found to be temperature independent in the entire range of temperature under study, regardless of the spectral weight function used in the analysis.

VI. SUMMARY OF CONCLUSIONS AND DISCUSSION

Well-defined spin-wave excitations have been observed in amorphous rapidly-quenched samples of $Fe_{100-x}B_x$ ($x=14$ and 18) at small wave vectors ($q\leq0.14$ $Å^{-1}$) at all temperatures studied ($T\leq0.92T_C$). The spin-wave excitation spectra were well described by a quadratic dispersion relation in q, with a very small energy gap. The spin-wave stiffness parameter D showed a temperature dependence consistent with the $T^{5/2}$ dependence predicted (at low temperatures) from models that account for magnon-magnon interactions. However, the $T=0$ stiffness parameter $D(0)$ (also referred in this paper as D_{SW}) is almost twice as large as the value D_m derived from low temperature magnetization measurements. The comparison of the $D(T)/D(0)$ versus $(T/T_C)^{5/2}$ curves of several amorphous systems suggests that the renormalization of the spin-wave stiffness parameter with temperature is more dramatic in Invar than in the non-Invar systems. This is reflected in the relatively large coefficient A' of Eq. (16). Within the Heisenberg ferromagnet model this means that the range of interaction, defined as the second moment of the exchange interaction $\langle r^2\rangle$, is relatively large in Invar systems.

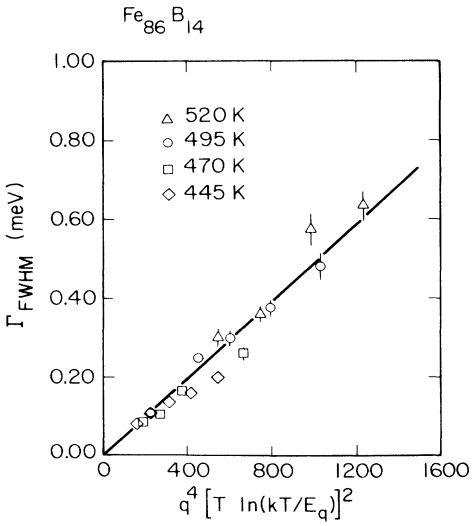

FIG. 12. Γ_q (FWHM of the damped harmonic oscillator spectral weight function) vs $q^4[T\ln(k_BT/E_q)]^2$ for $Fe_{86}B_{14}$-II. The solid curve is the same as in Fig. 11.

However, a long-range exchange interaction in amorphous systems seems to be unphysical due to the strong disorder present. Another interpretation of the rather large value of the coefficient A' is that there might be additional excitations in the Invar systems that contribute to the rapid decrease of D with increasing temperature. These excitations would evidently have the same density of states as the spin-wave excitations, and might be of the kind suggested by Vaks *et al.*[16] for the coupling of longitudinal spin fluctuations with spin waves. At lower temperatures, longitudinal modes might be significant due to the mechanism proposed by Continentino and Rivier[32] for systems where there is strong competition between ferromagnetic and antiferromagnetic exchange interactions.

A detailed analysis of the wave-vector and temperature dependence of the spin-wave linewidths has been performed on $Fe_{86}B_{14}$. At all temperatures and q's studied, the linewidth data were in agreement with the prediction of the two-magnon interaction theory of the Heisenberg ferromagnet. Thus there was no indication of the empirical q^2 dependence of the spin-wave linewidth suggested by Ishikawa and collaborators. The relatively rapid decrease of the magnetization with temperature in these Invar systems appears to derive from additional excitations in the system, as suggested from our analysis of the temperature dependence of the stiffness parameter, and not from anomalous spin-wave linewidths.

Further experiments are needed in order to single out the nature of these excitations. In particular, neutron polarized beam experiments at low temperatures would be useful to determine if there are longitudinal spin fluctuation modes as predicted by Continentino and Rivier. Higher incident neutron energy experiments would also be useful to increase the wave-vector range of the experiments and hence study the contribution of higher-order terms in the spin-wave dispersion relation.[67]

ACKNOWLEDGMENTS

We would like to express our gratitude to the people that helped us in the different stages of this project. In particular, we would like to thank R. W. Erwin and J. A. Gotaas at the National Bureau of Standards, and M. Hagen and R. M. Nicklow at Oak Ridge National Laboratory. We would also like to thank D. Huber for his valuable comments. The research at the University of Maryland was supported by the National Science Foundation under Grants Nos. DMR 83-19936 and DMR 86-20269. The research at Oak Ridge National Laboratory was sponsored by the U.S. Department of Energy under Contract No. DE-AC05-84OR21400 with Martin Marietta Energy Systems, Inc.

---

*Present address: Solid State Division, Oak Ridge National Laboratory, Oak Ridge, TN 37831.

[1]For a review of the spin dynamics of amorphous systems see, J. W. Lynn and J. J. Rhyne, *Spin Dynamics of Amorphous Magnets*, in *Spin Waves and Magnetic Excitations*, edited by A. S. Borovik-Romanov and S. K. Sinha (North-Holland, Amsterdam, in press), Chap. 15.

[2]Y. Nakamura, IEEE Trans. Magn. **MAG-12**, 278 (1976).

[3]J. A. Fernandez-Baca, J. W. Lynn, J. J. Rhyne, and G. E. Fish, J. Appl. Phys. **57**, 3545 (1985); Physica **136B**, 53 (1986).

[4]The terms spin wave and magnon are used interchangeably in this paper.

[5]J. Hubbard and J. L. Beeby, J. Phys. C **2**, 556 (1969).

[6]T. Kaneyoshi, J. Phys. C **5**, L65 (1972); **5**, 3504 (1972); J. Phys. Soc. Jpn. **45**, 1835 (1978).

[7]M. A. Continentino and N. Rivier, Physica **86-88B**, 793 (1977).

[8]U. Krey, J. Magn. Magn. Mater. **6**, 27 (1977).

[9]F. J. Dyson, Phys. Rev. **102**, 1217 (1956); **102**, 1230 (1956).

[10]W. Marshall and G. Murray, J. Phys. C **2**, 539 (1969).

[11]D. L. Huber, and R. P. Siemann, Solid State Commun. **17**, 769 (1975).

[12]W. Marshall, in *Proceedings of the Eight International Conference of Low Temperature Physics*, edited by R. O. Davies (Butterworths, London, 1963), p. 215.

[13]T. Izuyama, Phys. Lett. **9**, 293 (1964).

[14]A. B. Harris, Phys. Rev. **175**, 674 (1968); **184**, 606 (1969).

[15]V. N. Kashcheev and M. A. Krivoglaz, Fiz. Tverd. Tela (Leningrad) **3**, 1541 (1961) [Sov. Phys.—Solid State **3**, 1117 (1961)].

[16]V. G. Vaks, A. I. Larkin, and S. A. Pikin, Zh. Eksp. Teor. Fiz. **53**, 1089 (1967) [Sov. Phys.—JETP **26**, 647 (1968)].

[17]J. D. Axe, G. Shirane, T. Mizoguchi, and K. Yamauchi, Phys. Rev. B **15**, 2763 (1977).

[18]J. A. Tarvin, G. Shirane, R. J. Birgeneau, and H. S. Chen, Phys. Rev. B **17**, 241 (1978).

[19]Z. Xianyu, Y. Ishikawa, and S. Onodera, J. Phys. Soc. Jpn. **51**, 1799 (1982).

[20]V. A. Singh and L. M. Roth, J. Appl. Phys. **49**, 1642 (1978).

[21]H. Mano, J. Phys. Soc. Jpn. **51**, 3157 (1982).

[22]R. S. Ishkakov, Fiz. Tverd. Tela (Leningrad) **19**, 3 (1977) [Sov. Phys.—Solid State **19**, 1 (1977)].

[23]J. A. Fernandez-Baca, J. W. Lynn, J. J. Rhyne, and G. E. Fish, J. Appl. Phys. **61**, 3406 (1987).

[24]S. W. Lovesey, *Theory of Neutron Scattering from Condensed Matter* (Clarendon, Oxford, 1984), Vol. 2, Chap. 9.

[25]R. W. Erwin, J. W. Lynn, J. J. Rhyne, and H. S. Chen, J. Appl. Phys. **57**, 3473 (1985); and unpublished.

[26]P. W. Mitchell, R. A. Cowley, and R. Pynn, J. Phys. C **17**, L875 (1984).

[27]Y. Ishikawa, K. Tajima, Y. Noda, and N. Wakabayashi, J. Phys. Soc. Jpn. **48**, 1097 (1980).

[28]S. Onodera, Y. Ishikawa, and K. Tajima, J. Phys. Soc. Jpn. **50**, 1513 (1981); Y. Ishikawa, S. Onodera, and K. Tajima, J. Magn. Magn. Mater. **10**, 183 (1979).

[29]S. Onodera, Y. Ishikawa, M. Shiga, Z. Xianyu, and Y. Nakamura, J. Phys. Soc. Jpn. **9**, 2705 (1982).

[30]Z. Xianyu, Y. Ishikawa, S. Ishio, and M. Takahashi, J. Phys. F **15**, 1787 (1985).

[31]Y. Ishikawa, K. Yamada, K. Tajima, and K. Fukamichi, J. Phys. Soc. Jpn. **50**, 1958 (1981).

[32]M. A. Continentino and N. Rivier, J. Phys. F **9**, L145 (1979);

N. Rivier and M. A. Continentino, J. Magn. Magn. Mater. **15-18**, 1419 (1980).
[33]E. P. Wohlfarth, J. Appl. Phys. **39**, 1061 (1968); J. Magn. Magn. Mater. **10**, 120 (1979).
[34]E. D. Thompson, E. P. Wohlfarth, and A. C. Bryan, Proc. Phys. Soc. London **83**, 59 (1964).
[35]V. E. Rode, R. Gerrmann, and N. V. Mikhailova, Zh. Eksp. Teor. Fiz. **49**, 3 (1965) [Sov. Phys.—JETP **22**, 1 (1966)].
[36]I. Nakai, F. Ono, and O. Yamada, J. Phys. Soc. Jpn. **48**, 1105 (1980).
[37]R. W. Cochrane and G. M. Graham, Can. J. Phys. **48**, 264 (1970).
[38]O. Yamada, M. Mimura, H. Maruyama, I. Nakai, S. Ishio, and M. Takahashi, J. Magn. Magn. Mater. **54-57**, 250 (1986); I. Nakai, O. Yamada, M. Mimura, S. Ishio, and M. Takahashi, J. Phys. F (to be published).
[39]E. Babic, Z. Marohnic, and E. P. Wohlfarth, Phys. Lett. **95A**, 335 (1983).
[40]R. Hasegawa and R. Ray, Phys. Rev. B **20**, 211 (1979).
[41]M. C. Narasimhan, U. S. Patent 4,331,739 (1982).
[42]M. G. Scott, in *Amorphous Metal Alloys,* edited by F. E. Luborsky (Butterworths, London, 1983), Chap. 10.
[43]S. M. Shapiro and N. J. Chesser, Nucl. Instrum. Methods **101**, 183 (1972).
[44]M. J. Cooper and R. Nathans, Acta Cryst. **23**, 357 (1967).
[45]N. J. Chesser and J. D. Axe, Acta Cryst. A **29**, 160 (1973).
[46]Z. Xianyu, Y. Ishikawa, T. Fukunaga, and N. Watanabe, J. Phys. F **15**, 1799 (1985).
[47]J. J. Rhyne, G. E. Fish, and J. W. Lynn, J. Appl. Phys. **53**, 2316 (1982).
[48]R. Weber and P. E. Tannenwald, Phys. Rev. **140**, A498 (1965).
[49]M. Bloch, J. Appl. Phys. **34**, 1151 (1963).
[50]H. A. Mook and J. W. Lynn, Phys. Rev. B **29**, 4056 (1984); S. C. Yu, J. W. Lynn, and W. H. Li (unpublished). Metglas is Allied Corporation's registered trademark for amorphous alloys of metals.
[51]A. Z. Menshikov, A. Chamberod, and M. Roth, Solid State Commun. **44**, 243 (1982).
[52]J. J. Rhyne and G. E. Fish, J. Appl. Phys. **57**, 3407 (1985).
[53]R. Krishnan, K. V. Rao, and H. H. Liebermann, J. Appl. Phys. **55**, 1823 (1984).
[54]K. Shirakawa, S. Ohnuma, M. Nose, and T. Masumoto, IEEE Trans. Magn. **MAG-16**, 910 (1980).
[55]Y. Ishikawa, Physica **136B**, 451 (1985).
[56]S. N. Kaul, Phys. Rev. B **24**, 6550 (1981).
[57]R. J. Birgeneau, J. A. Tarvin, G. Shirane, E. M. Gyorgy, R. C. Sherwood, and H. S. Chen, Phys. Rev. B **18**, 2192 (1978).
[58]J. A. Fernandez-Baca, J. J. Rhyne, and G. E. Fish, J. Magn. Magn. Mater. **54-57**, 289 (1986).
[59]W. Dmowski, H. Matyja, and R. Puzniak, J. Magn. Magn. Mater. **41**, 188 (1984).
[60]W. Minor, B. Lebech, K. Clausen, and W. Dmowski, in *Rapidly Quenched Metals,* edited by S. Steeb and H. Warlimont (Elsevier, Amsterdam, 1985), p. 1149.
[61]Y. Ishikawa, Z. Xianyu, S. Onodera, S. Ishio, and M. Takahashi, in *Proceedings of the Fourth International Conference on Rapidly Quenched Materials,* edited by T. Masumoto and K. Suzuki (Japan Institute of Metals, Sendai, 1982), p. 1093.
[62]J. D. Axe, L. Passell, and C. C. Tsuei, in Magnetism and Magnetic Materials—1974, Proceedings of the 20th Annual Conference on Magnetism and Magnetic Materials, AIP Conf. Proc. No. 24, edited by C. D. Graham, G. H. Lander, and J. J. Rhyne (AIP, New York, 1975), p. 119.
[63]H. A. Mook and C. C. Tsuei, Phys. Rev. B **16**, 2184 (1977).
[64]H. Grimsditch, A. Malozemoff, and A. Brunsch, Phys. Rev. Lett. **43**, 711 (1979).
[65]K. Fukamichi, M. Kikuchi, S. Arakawa, and T. Masumoto, Solid State Commun. **23**, 955 (1977).
[66]A. K. Majumdar, V. Oestreich, and D. Weschenfelder, Phys. Rev. B **27**, 5618 (1983).
[67]The results presented in this paper were part of one of the authors' (J.A.F.) dissertation submitted to the Faculty of the Graduate School of the University of Maryland in partial fulfillment of the requirements for the degree of Doctor of Philosophy.